

## A DYNAMIC FINITE ELEMENT CODE FOR ANALYZING COLLAPSE BEHAVIORS OF FRAMED STRUCTURES UNDER SEISMIC LOADS

D. Isobe<sup>1</sup> and N. Katahira<sup>2</sup>

<sup>1</sup>Dept. of Eng. Mech. and Energy, Univ. of Tsukuba  
1-1-1 Tennodai Tsukuba-shi, Ibaraki 305-8573, Japan  
e-mail: isobe@kz.tsukuba.ac.jp

<sup>2</sup> College of Eng. Systems, Univ. of Tsukuba  
1-1-1 Tennodai Tsukuba-shi, Ibaraki 305-8573, Japan  
e-mail: e0311273@edu.esys.tsukuba.ac.jp

**Keywords:** Framed Structures, Seismic Load, Collapse Behavior, ASI-Gauss Technique, Finite Element Method.

**Abstract.** *A new dynamic finite element code to simulate collapse behaviors of structures under excitation at fixed points is developed using the ASI-Gauss technique. The technique is a modified version of the formerly developed Adaptively Shifted Integration (ASI) technique for the linear Timoshenko beam element, which computes highly accurate elasto-plastic solutions even with the minimum number of elements per member. The ASI-Gauss technique gains still higher accuracy especially in elastic range, by placing the numerical integration points of the two consecutive elements forming an elastically deformed member in such a way that stresses and strains are evaluated at the Gaussian integration points of the two-element member. Moreover, the technique can be used to express member fracture, by shifting the numerical integration point to an appropriate position and by releasing the resultant forces in the element simultaneously. The numerical code can be used to analyze dynamic behaviors of framed structures, initiating from elastic range to a total collapse. Simple numerical tests are conducted to verify the proposed code. Moreover, a seismic collapse analysis considering member fracture and contact is performed on a large-scale framed structure, and practical results are obtained in a reasonable short calculation time.*

## 1 INTRODUCTION

In the conventional design of a building, only static analysis in the horizontal and uniaxial directions is commonly carried out, in order to minimize calculation costs. This approach can ensure the structural strength of the building, if there is sufficient strength to support the load in the vertical direction. For a similar reason, the mass system model replaces the building layer in dynamic analysis, and the complicated dynamic behavior of the structure at the member level becomes difficult to be examined sufficiently. Therefore, the development of a more precise and more efficient dynamic analysis code is strongly desired.

Recently, significant advances in the field of computers have been eliminating the calculation cost restrictions, and various dynamic analysis codes are being developed. Among those codes, there are some codes applicable to dynamic collapse problems which contain strong nonlinearities and discontinuities, such as the Distinct Element Method (DEM) [1] or the Discontinuous Deformation Analysis (DDA) [2]. These codes have been applied to demolition analyses and seismic collapse analyses [3-8]. However, the above-mentioned discrete numerical methods are computationally intensive and need detailed modeling. Therefore, they are suitable only for detailed analyses of either two-dimensional or small three-dimensional models.

On the other hand, the Finite Element Method (FEM), which is based on continuum material equations, has been successfully applied to a wide range of engineering problems including structural analyses of large-scale structures. However, the FEM is generally limited to analyses of relatively small displacements and it needs complicated modifications to simulate fracture occurring in structural members or joints. The main objective of this study is to develop a finite element code, which can simulate dynamic behaviors with such strong nonlinearities and discontinuities and is efficiently applicable to seismic collapse analyses of framed structures.

Toi and Isobe developed the Adaptively Shifted Integration (ASI) technique [9,10] for the linear Timoshenko beam and the Bernoulli-Euler beam elements, which can be easily implemented into the existing finite element codes. In this technique, the numerical integration point is shifted immediately after the occurrence of a fully plastic section in the element so that a plastic hinge is formed exactly at that section. As a result, the ASI technique gives more precise elasto-plastic solutions than the conventional schemes, and has become able to simulate dynamic behaviors with strong nonlinearities by using only a small number of elements for a member. Structurally discontinuous problems have also become easily handled, by shifting the numerical integration point of the linear Timoshenko beam element to an appropriate position, and by releasing the resultant forces in the element simultaneously [11,12]. However, when the number of elements per member is very small, it still lacks accuracy in the elastic range compared to the converged solution, due to the low-order displacement function of the linear Timoshenko beam element.

To improve the accuracy in elastic range, Isobe and Lynn modified the ASI technique into an ASI-Gauss technique [13]. The accuracy in elastic range is improved by placing the numerical integration points of the two consecutive elements forming an elastically deformed member in such a way that stresses and strains are evaluated at the Gaussian integration points of the two-element member, where the accuracy of bending deformation is mathematically guaranteed for two-point integration. The rest of the shiftings are done according to the flow of the ASI technique.

In this study, the ASI-Gauss technique is implemented into the finite element code in order to develop a more precise and less-calculation-time-consuming seismic collapse analytical tool. The purpose of this study is to verify the validity of the ASI-Gauss technique in seismic collapse

analysis and to construct a highly efficient structural design tool for framed structures. Simple numerical tests are carried out to show the validity of the code, and an analysis involving member fracture and contact is performed on a large-scale framed structure to show the practicability of the scheme.

## 2 NUMERICAL METHOD

General concept of the ASI-Gauss technique in comparison with the ASI technique is explained in this section. Moreover, algorithms considering member fracture and elemental contact, and incremental kinematic equation for excitation at fixed points, are described.

### 2.1 ASI-Gauss technique

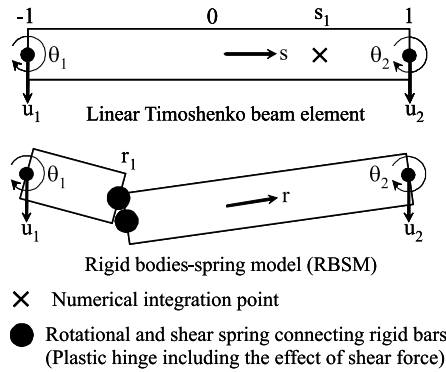


Figure 1: Linear Timoshenko beam element and its physical equivalent.

Figure 1 shows a linear Timoshenko beam element and its physical equivalence to the rigid bodies-spring model (RBSM). As shown in the figure, the relationship between the locations of the numerical integration point and the stress evaluation point where a plastic hinge is actually formed is expressed as [14]

$$r = -s \quad (1)$$

In the above equation,  $s$  is the location of the numerical integration point and  $r$  the location where stresses and strains are actually evaluated. We refer to  $r$  as the stress evaluation point later in this paper.  $s$  is a nondimensional quantity, which takes a value between -1 and 1.

In both the ASI and ASI-Gauss techniques, the numerical integration point is shifted adaptively when a fully plastic section is formed within an element to form a plastic hinge exactly at that section. When the plastic hinge is determined to be unloaded, the corresponding numerical integration point is shifted back to its normal position. Here, the normal position means the location where the numerical integration point is placed when the element acts elastically. By doing so, the plastic behavior of the element is simulated appropriately, and the converged solution is achieved with only a small number of elements per member. However, in the ASI technique, the numerical integration point is placed at the midpoint of the linear Timoshenko beam element, which is considered to be optimal for one-point integration, when the entire region of the element behaves elastically. When the number of elements per member is very small, solutions in the elastic range are not accurate since one-point integration is used to evaluate the low-order displacement function of the beam element.

The main difference between the ASI and ASI-Gauss techniques lies in the normal position of the numerical integration point. In the ASI-Gauss technique, two consecutive elements form-



Here,  $f_y$  is the yield function, and  $M_x$ ,  $M_y$ ,  $N$  and  $M_z$  are the bending moments around the x- and y- axes, axial force and torsional moment, respectively. Those with the subscript 0 are values that result in a fully plastic section in an element when they act on a cross section independently. The effect of shear force is neglected in the yield function.

## 2.2 Member fracture and contact algorithm

A plastic hinge is likely to occur before it develops to a member fracture, and the plastic hinge is expressed by shifting the numerical integration point to the opposite end of the fully-plastic section. Accordingly, the numerical integration point of the adjacent element forming the same member is shifted back to its midpoint where it is appropriate for one-point integration. Figure 3 shows the locations of numerical integration points for each stage in the ASI-Gauss technique.

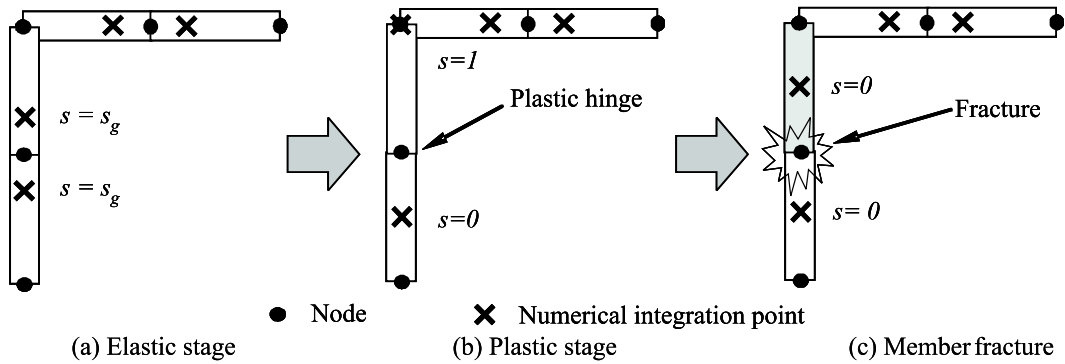


Figure 3: Locations of numerical integration points in each stage.

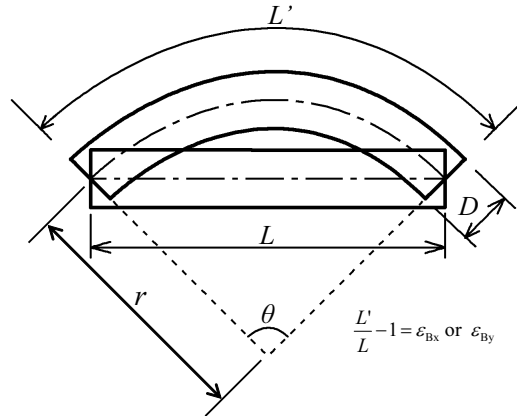


Figure 4: Definition of bending strain.

Member fracture is determined, in this study, by means of bending strain and axial strain occurred in the elements. By assuming that a pin-supported element is deformed as shown in Fig. 4, the initial length  $L$  and the maximum deformed length  $L'$  of the element are expressed as

$$L = 2r \sin \frac{\theta}{2} \quad (5a)$$

$$L' = \left(r + \frac{D}{2}\right)\theta \quad (5b)$$

where  $D$  is the member width,  $r$  and  $\theta$  are the radius and angle of the bending deformation, respectively. Bending strain  $\varepsilon_B$  is defined using Eqs. (5) as

$$\varepsilon_B = \frac{L'}{L} - 1 = \frac{D\theta}{2L} + \frac{\theta}{2\sin(\theta/2)} - 1 \quad (6)$$

Here, two angles of bending deformation around the x- and y- axes can be written as

$$\theta_x = |\kappa_x|L \quad (7a)$$

$$\theta_y = |\kappa_y|L \quad (7b)$$

where  $\kappa_x$  and  $\kappa_y$  are the curvatures around the x- and y- axes, respectively. Substituting Eqs. (7) into Eq. (6) yields to the following equations that calculate bending strains around the x- and y- axes.

$$\varepsilon_{Bx} = \frac{D}{2}|\kappa_x| + \frac{|\kappa_x|L}{2\sin(|\kappa_x|L/2)} - 1 \quad (8a)$$

$$\varepsilon_{By} = \frac{D}{2}|\kappa_y| + \frac{|\kappa_y|L}{2\sin(|\kappa_y|L/2)} - 1 \quad (8b)$$

Member fracture is determined when the sum of bending strains  $\varepsilon_{Bx}$ ,  $\varepsilon_{By}$  and axial strain  $\varepsilon_z$  satisfies the following condition.

$$\varepsilon_{z0} \leq \varepsilon_{Bx} + \varepsilon_{By} + \varepsilon_z \quad (9)$$

Here,  $\varepsilon_{z0}$  is the ultimate tensile strain of the member material.

Contact determination is done by examining the geometrical locations of the elements and once two elements are determined to be in contact, they are bound with a total of four gap elements between the nodes.

### 2.3 Incremental kinematic equation

The incremental kinematic equation for a structure under excitation at fixed points, which is used in this paper, is as follows:

$$[M_1]\{\Delta\ddot{u}\} + [M_2]\{\Delta\ddot{u}_b\} + [K_1]\{\Delta u\} + [K_2]\{\Delta u_b\} = 0 \quad (10)$$

The subscript '1' indicates the coupled terms between free nodal points, '2' indicates the coupled terms between free nodal and fixed nodal points, and 'b' indicates the components at fixed nodal points.  $[M]$  is the mass matrix, and vectors  $\{\Delta\ddot{u}\}$  and  $\{\Delta u\}$  are the nodal acceleration increment and the nodal displacement increment, respectively.

Under the assumption that the displacements at free nodal points are estimated by adding quasi-static displacement increments  $\{\Delta u_s\}$  and dynamic displacement increments  $\{\Delta u_d\}$ , the displacements at free nodal points are given as

$$\{\Delta u\} = \{\Delta u_s\} + \{\Delta u_d\} \quad (11)$$

$\{\Delta u_s\}$  is evaluated, by neglecting inertia force, as follows:

$$\{\Delta u_s\} = -[K_1]^{-1}[K_2]\{\Delta u_b\} \quad (12)$$

Substituting Eqs. (11) and (12) into Eq. (10), the following equation is obtained:

$$[M_1]\{\Delta\ddot{u}_d\} + [K_1]\{\Delta u_d\} = ([M_1][K_1]^{-1}[K_2] - [M_2])\{\Delta\ddot{u}_b\} \quad (13)$$

In this scheme, equivalent forces are calculated by substituting nodal acceleration increments at fixed points into the right side of the above equation. Damping matrices are not considered in this study.

### 3 NUMERICAL ESTIMATIONS

To verify the numerical code using the ASI-Gauss technique, simple elasto-plastic response analyses under seismic excitation are performed. In the analyses, we use the following three schemes to verify the accuracy of the ASI-Gauss technique: (a) a conventional finite element scheme in which the numerical integration point of each element is fixed at its midpoint; (b) the ASI technique; and (c) the ASI-Gauss technique. Figure 5 shows the analyzed space frame with its dimensions, physical properties and material constants. An EW component of JMA Kobe seismic wave is multiplied by 1.5 for the amplitude as shown in Fig. 6, and is subjected at the fixed points according to Eqs. (10) to (13). An implicit solution scheme using Newmark's  $\beta$  method ( $\beta = 4/9$  and  $\delta = 5/6$  is used to consider numerical damping), updated Lagrangian formulation, and a consistent mass matrix are adopted in the analyses.

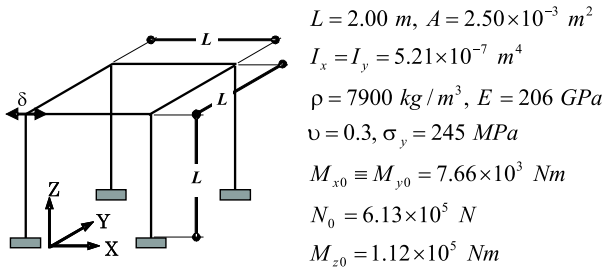


Figure 5: Analyzed model.

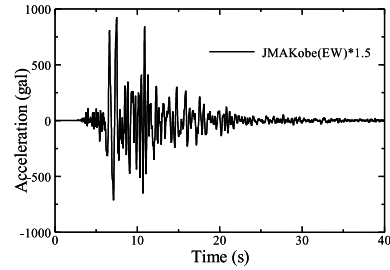


Figure 6: Input seismic wave (EW, JMA-Kobe).

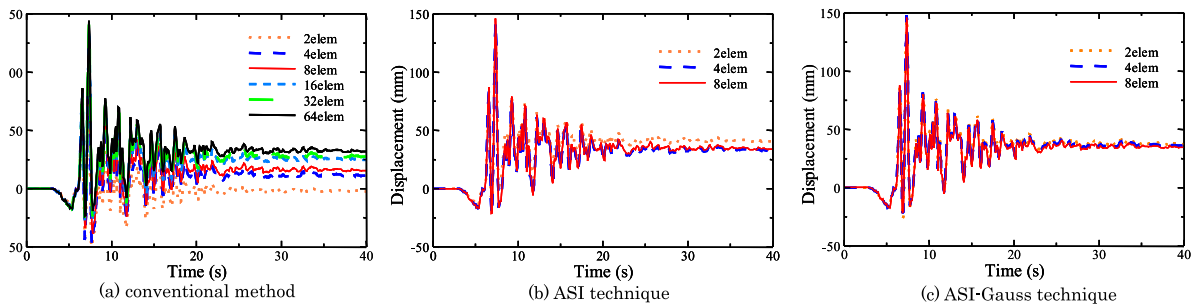


Figure 7: Comparison of the numerical accuracies between three schemes.

Figure 7 shows the results of the analyses. Since plastic hinges are expressed only at the midpoints of the elements, the conventional scheme shows a very slow convergence and it still does not converge even when the 64-element modeling is used. The ASI technique gives comparatively better results than the conventional scheme. However, the two-element modeling yet does not give converged solution, since the elements lack with accuracy in the elastic range.

On the other hand, the ASI-Gauss technique shows a very fast convergence and a converged solution is obtained with the minimum subdivision, since the stress evaluation points in the elements are adaptively controlled in both elastic and plastic ranges. The three-dimensional excitation gave the same tended results.

#### 4 SEISMIC COLLAPSE ANALYSIS OF A LARGE-SCALE FRAMED STRUCTURE

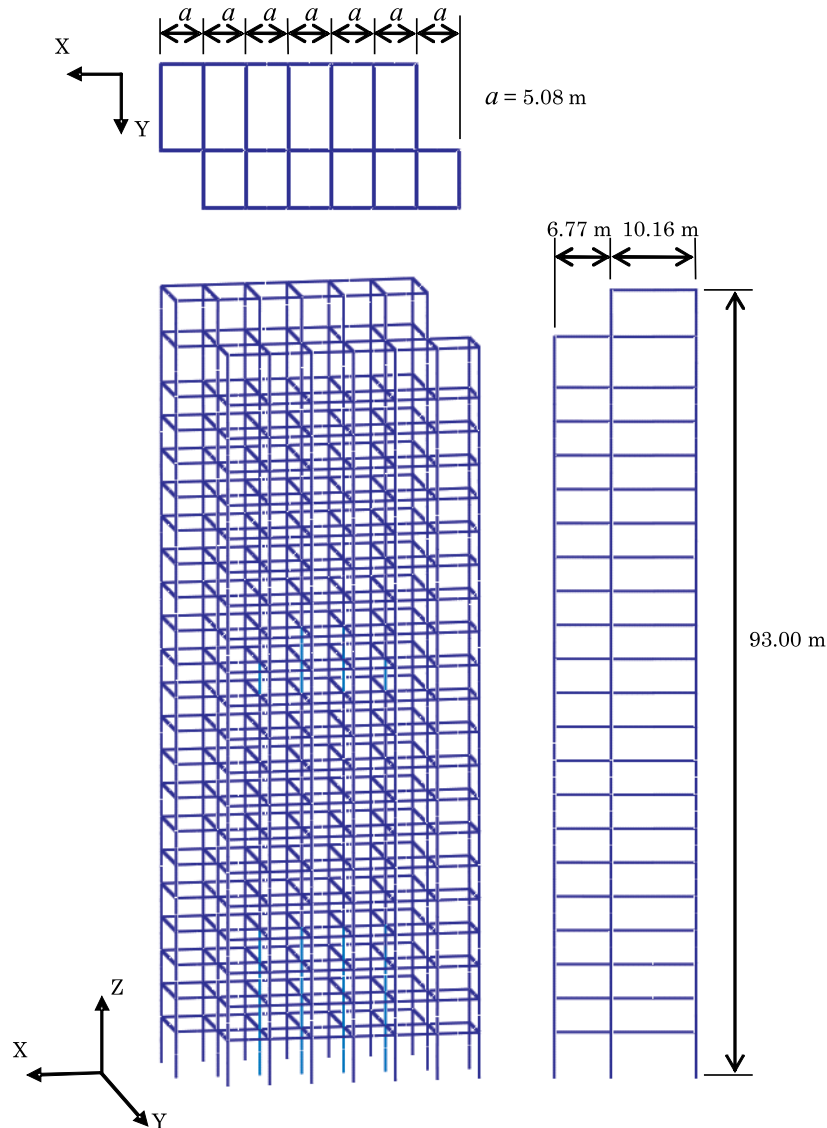


Figure 8: Analyzed model.

A seismic collapse analysis is carried out on a 22-story steel framed structure as shown in Fig. 8. Member list of the structure is shown in Table 1. We assumed a structure with lower stiffness and longer natural period to see the effect of a large seismic wave in such condition. The natural periods of the structure are 13 s to the X-direction, and 20 s to the Y-direction. EW and NS components of JMA Kobe seismic wave (Fig. 6 and Fig. 9), also multiplied by 1.5 for the amplitude, are subjected orthographically (EW to X-direction, NS to Y-direction) at the fixed points on the ground floor. Dead load for each floor is assumed as  $200 \text{ kg/m}^2$ , and a value

of 0.22 is used for  $\varepsilon_{z0}$  in Eq. (9). The time increment is set to 5 ms and the calculation is done for a total of 8000 steps. The calculation takes approximately 30 CPU minutes with a personal computer (Core2 DUO E6300, 1.86 GHz CPU $\times$ 2, 3 GB RAM).

Member	Spec. (material)
Column (1F-11F)	-250*250*9 (SN490)
Column (11F-22F)	-200*200*6 (SN490)
Beam	H-200*200*8*12 (SN490)

Table 1: Member list.

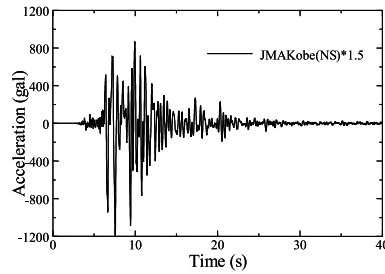


Figure 9: Input seismic wave (NS, JMA-Kobe).

The numerical result is shown in Fig. 10. A total of six colors are used to demonstrate the tendency of the elements to yielding. The numbers in the color palette indicate the values of  $f_y$  in Eq. (4). Red color ( $f_y = 1.0$ ) means a plastic hinge is formed within the element. Fractured elements are excluded from the figure. Although the maximum amplitude of the input seismic wave is observed between 5 s to 12 s, only the ground level columns are yielded during the period. However, a so-called incremental collapse continues to proceed in the columns due to small excitations after the period, and finally, the structure begins to collapse totally after 26 s when excitations are decreased to an appearingly small amount. In this case, a difference between the natural period of the structure and the seismic wave led to a stress concentration on ground level columns, which reduced the total vertical resistant force of the structure itself. The collapse process can be confirmed in detail by observing the story-shear and drift angle relations of one of the columns on the ground floor (Fig. 11) and the drift angle time histories (Fig. 12). By observing the drift angle values, it is clear that the EW component (X-direction) of the seismic wave played a main role in the total collapse behavior of the structure. It may also be said that the member fracture and contact algorithms have succeeded to express a realistic phenomenon of the total collapse.

## 5 CONCLUSIONS

In this paper, a nonlinear finite element code using the ASI-Gauss technique was developed, in order to analyze seismic collapse problems including structural discontinuities. The fracture of a section was modeled by shifting the numerical integration point with simultaneous release of the resultant forces. The proposed code was improved by considering the contact between members in order to obtain results that agree more closely with the actual behavior. The code gives accurate and practically realistic results in a short calculation time, which may be valid

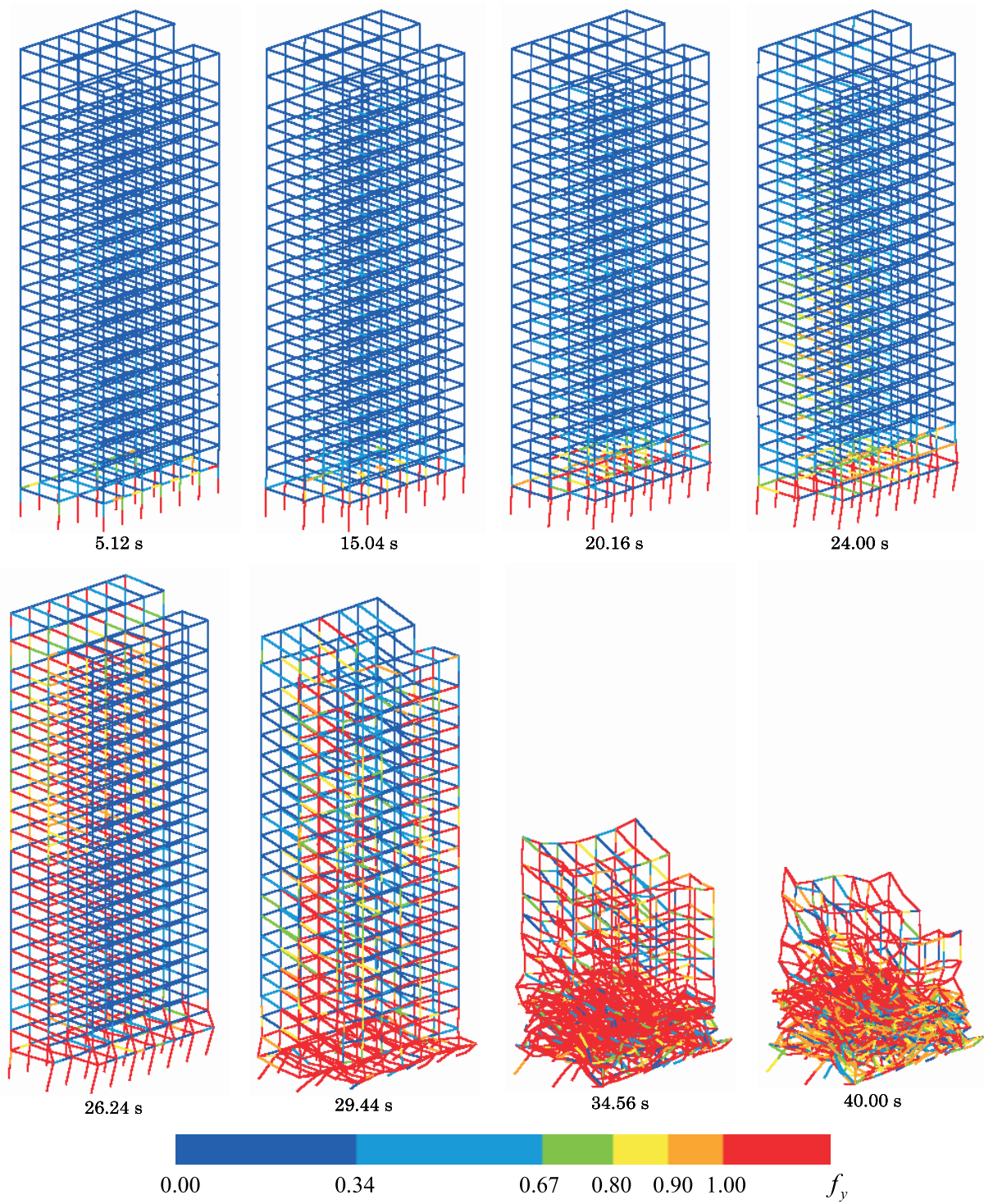


Figure 10: Seismic collapse analysis of a large-scale framed structure.

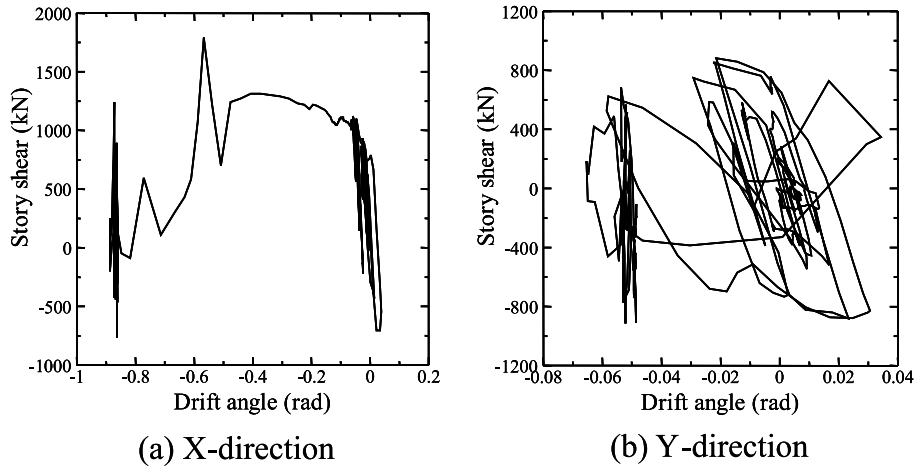


Figure 11: Story-shear and drift angle relations on the ground floor.

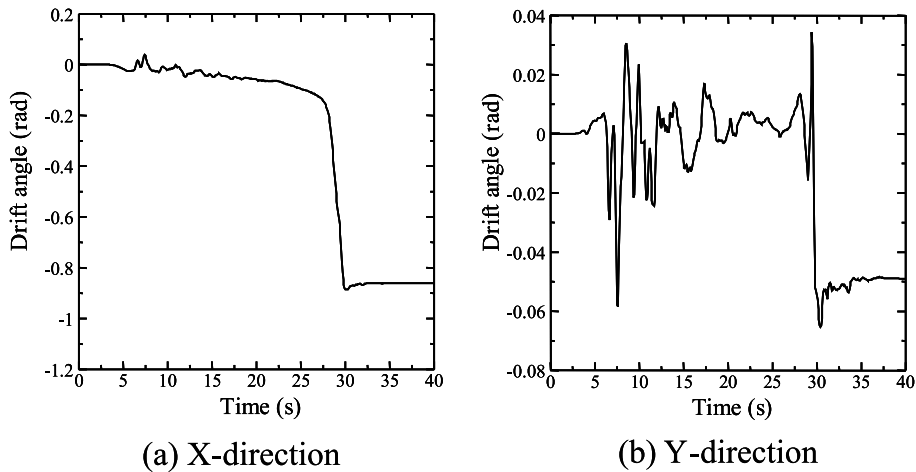


Figure 12: Time histories of drift angles.

when used in a numerical estimation of the seismic design of large-scale framed structures. However, the damping matrices, as well as more detailed member properties, should also be considered in the future studies to improve the accuracy.

## 6 ACKNOWLEDGEMENT

This research is done partially as a trustee project of National Research Institute for Earth Science and Disaster Prevention (NIED), Japan.

## REFERENCES

- [1] P.A. Cundall, A Computer Model for simulating Progressive, Large-scale Movement in Blocky Rock System, *Proceedings of the International Symposium on Rock Mechanics*, **II-8**, 129-136, 1971.
- [2] G.H. Shi and R.E. Goodman, Discontinuous Deformation Analysis, *Proceedings of 25th U.S. Symposium on Rock Mechanics*, 269-277, 1984.

- [3] K. Meguro and M. Hakuno, Simulation of Collapse Process of Structures due to Earthquake, *Proceedings of Symposium on Computational Methods in Structural Engineering and Related Fields*, **15**, 325-330, 1991. [in Japanese]
- [4] M. Itoh, N. Yoshida, N. Utagawa and I. Kondo, Simulation of Blast Demolition of Reinforced Concrete Buildings, *Proceedings of the Third World Congress on Computational Mechanics*, 1152-1153, Chiba, Japan, August 1-5, 1994.
- [5] M.Y. Ma, P. Barbeau and D. Penumadu, Evaluation of active thrust on retaining walls using DDA, *Journal of Computing in Civil Engineering*, **1**, 820-827, 1995.
- [6] I. Kondo, N. Utagawa, M. Ito and N. Yoshida, Numerical Method to Simulate Collapse Behavior in Blasting Demolition of Space Framed Structure, *Proceedings of the 13th Symposium on Computer Technology of Information, Systems and Applications*, 49-54, 1990. [in Japanese]
- [7] E. Yarimer, Demolition by Controlled Explosion as a Dynamical Process, *Structures under Shock and Impact*, 411-416, 1989.
- [8] N. Tosaka, Y. Kasai and T. Honma, Computer Simulation for Felling Patterns of Building, *Demolition Methods and Practice*, 395-403, 1988.
- [9] Y. Toi and D. Isobe, Adaptively Shifted Integration Technique for Finite Element Collapse Analysis of Framed Structures, *International Journal for Numerical Methods in Engineering*, **36**, 2323-2339, 1993.
- [10] Y. Toi and D. Isobe, Finite Element Analysis of Quasi-static and Dynamic Collapse Behaviors of Framed Structures by the Adaptively Shifted Integration Technique, *Computers and Structures*, **58(5)**, 947-955, 1996.
- [11] D. Isobe and Y. Toi, Analysis of Structurally Discontinuous Reinforced Concrete Building Frames Using the ASI Technique, *Computers and Structures*, **76(4)**, 471-481, 2000.
- [12] D. Isobe and M. Tsuda, Seismic Collapse Analysis of Reinforced Concrete Framed Structures Using the Finite Element Method, *Earthquake Engineering and Structural Dynamics*, **32(13)**, 2027-2046, 2003.
- [13] D. Isobe and K.M. Lynn, A Finite Element Code for Structural Collapse Analyses of Framed Structures Under Impact Loads, *Proceedings of the 4th European Congress on Computational Methods in Applied Sciences and Engineering (ECCOMAS 2004)*, Jyväskylä, Finland, July 24-28, 2004.
- [14] Y. Toi, Shifted Integration Technique in One-Dimensional Plastic Collapse Analysis Using Linear and Cubic Finite Elements, *International Journal for Numerical Methods in Engineering*, **31**, 1537-1552, 1991.
- [15] W.H. Press, S.A. Teukolsky, W.T. Vetterling and B.P. Flannery, *Numerical Recipes in FORTRAN: The Art of Scientific Computing, 2nd Edition*. Cambridge University Press, 1992.